This full text paper was peer reviewed at the direction of IEEE Communications Society subject matter experts for publication in the IEEE ICC 2009 proceedings

Distributed Quality-Lifetime Maximization in Wireless Video Sensor Networks

Eren Gürses*, Yuan Lin†, Raouf Boutaba*
*School of Computer Science, University of Waterloo, Waterloo, ON N2L 3G1, Canada
†Center for Quantifiable QoS in Communication Systems, NTNU, N-7491, Trondheim, Norway
{egurses, rboutaba}@uwaterloo.ca, yuan.lin@q2s.ntnu.no

***Abstract*—Owing to the availability of low-cost and low-power CMOS cameras, Wireless Video Sensor Networks (WVSN) has recently become a reality. However video encoding is still a costly process for energy and capacity constrained sensor nodes and its optimal joint control with the communication protocols has a direct impact on the network lifetime. In this paper we propose a distributed *quality-lifetime* control algorithm where quality is simply measured by the visual signal quality. In order to formulate the quality-lifetime problem, we consider the Power-Rate-Distortion (P-R-D) model of the video encoder together with the rate control, medium access and routing functions of the underlying communication protocol and formulate the problem as a Generalized Network Utility Maximization (GNUM) problem. Then we construct a distributed solution based on duality and proximal point methods with necessary convergence analysis. Simulation results support that optimal quality-lifetime control is possible through the proposed distributed algorithm, where the desired point of operation is simply adjusted by the sink via a configuration parameter.**

I. Introduction

Wireless video sensor networks (WVSN) have drawn significant amount of attention in the recent years due to both numerous potential application areas and enhancements they offer to existing WSN applications, such as video surveillance, battlefield awareness, environmental monitoring and industrial process control [1]. Due to the unattended and energy-capacity constrained nature of wireless sensor networks, the design of distributed, energy efficient, self-organizing and optimizing algorithms and communication protocols have become the typical challenges in the recent years. A common goal of all these efforts is to maximize the network lifetime while accomplishing the given task which is generally decided by the measure of utility obtained from the network. In WVSNs a typical utility measure would be the sum of sensor-to-sink Signal-to-Noise-Ratio (SNR) which reflects the visual signal quality and increases with the amount of data communicated to the sink. However, higher data rate entails higher energy dissipation in the sensor nodes for capturing, processing and communicating video to the sink results in a shorter network lifetime. Hence the design of a quality-lifetime optimization framework for WVSN necessitates the proper modeling of both the video encoding process and the underlying communication mechanisms.

There has been some WVSN prototypes introduced in the recent years [1]. These works focus on practical and architectural aspects and have not considered the distributed system optimization. In [5], authors propose a distributed network lifetime maximization scheme considering video encoder model together with several communication layers. However they use distortion as a constraint not the objective function which may lead to problems with no feasible solution. In [4] authors propose a Generalized Network Utility Maximization (GNUM) based approach to solve the quality-lifetime maximization problem. However their work is not for video sensors and do not employ any Power-Rate-Distortion (P-R-D) model. Furthermore the proposed route selection algorithm continuously oscillates due to the discontinuous mapping from dual variables to primal ones. In this work we consider the P-R-D model of the video encoding process together with the underlying communication protocol functions such as rate control, medium access and route selection, and formulate the problem as a quality-lifetime maximization problem based on GNUM. Then we devise a low complexity and distributed algorithm based on duality and proximal point methods [6], [8] to solve it and provide a thorough convergence analysis which gives the bounds on the selection of step sizes that guarantee the convergence.

In Sec. II we describe the system architecture and the GNUM based formulation. In Sec. III we introduce the distributed quality-lifetime maximization algorithm together with the convergence analysis. In Sec. IV we present the simulation results and then conclude in Sec. V.

II. System Architecture

Considering a wireless video sensor network with single sink, let $\mathcal{N}$, $\mathcal{S}$, $\mathcal{L}$ and $\mathcal{R}(s)$ respectively denote the set of all nodes, source nodes, links and routes available to source s. Each sensor s generates data at a rate of y_s b/s transmitted over a set of routes $r \in \mathcal{R}(s)$ at rates x_r where $y_s = \sum_{r \in \mathcal{R}(s)} x_r$. Each link $l \in \mathcal{L}$ has a fixed capacity of c_l b/s.

A. Power-Rate-Distortion Model

In a typical WSN node, power is consumed either at the sensor stage for sensing and processing or at the radio stage for communication. In this section we formulate the processing power consumption at the sensor stage through a power-rate-distortion (P-R-D) model [3] where the communication power is later considered in Section II-C. An active video sensor captures and compresses the signal by introducing coding distortion $D_s(\sigma_s, y_s)$ given by (1) as a function of bit rate y_s

978-1-4244-3435-0/09/$25.00 ©2009 Crown

(in bits per pixel) and I (intra), P (inter) video coding mode rates σ_s, $1-\sigma_s$. In the rest of the paper we ignore the additional distortion due to channel losses by assuming the use of channel coding techniques to provide desirable receiver bit error rate (BER). In (1), $\delta_s^{(I)}$, $\delta_s^{(P)}$, γ_I, γ_P are given as variance and model accuracy constants for I and P-coding modes respectively and $k(\sigma_s,\gamma_I,\gamma_P) \triangleq \frac{\sigma_s}{\gamma_I}+\frac{1-\sigma_s}{\gamma_P}$ is defined.

$$D_s(\sigma_s,y_s)=k(\sigma_s,\gamma_I,\gamma_P)\left[(\delta_s^{(I)}\gamma_I)^{\frac{\sigma_s}{\gamma_I}}(\delta_s^{(P)}\gamma_P)^{\frac{1-\sigma_s}{\gamma_P}}2^{-2y_s}\right]^{\frac{1}{k(\sigma_s\gamma_I\gamma_P)}} \quad (1)$$

However, in (1) power information is implicit and available through I, P mode coding power parameters $p_s^{(I)}$, $p_s^{(P)}$ and I coding mode rate σ_s. Assuming $p_s^{(I)}$ and $p_s^{(P)}$ to be constants, we can write the encoder power as a function of σ as $p_s=\sigma_s p_s^{(I)}+(1-\sigma_s)p_s^{(P)}$. After defining $\omega_s=p_s^{(P)}/(p_s^{(P)}-p_s^{(I)})$ and solving for σ_s, I-coding mode rates are found as $\sigma_s = \omega_s(1-p_s/p_s^{(P)})$ once p_s is known. Now we can simplify the distortion model in (1) by setting $\gamma_I=\gamma_P=1$ which implies $k(\sigma_s,\gamma_I,\gamma_P) \triangleq 1$ and obtain $D_s(\sigma_s,y_s)=\delta_s^{(P)}\left(\delta_s^{(I)}/\delta_s^{(P)}\right)^{\sigma_s}2^{-2y_s}$. Afterwards, by replacing $\sigma_s = \omega_s(1-p_s/p_s^{(P)})$ we obtain the P-R-D model which explicitly relates distortion to the encoder rate y_s and encoder power p_s. By defining constants κ_s, η_s in (3) and $d_1=2\log 2$ the final form of the P-R-D model is obtained in (2) and later used in the quality-lifetime maximization problem in Sec. II-D.

$$D_s(p_s,y_s) = \eta_s \exp(-\kappa_s p_s)\exp(-d_1 y_s) \quad (2)$$

$$\kappa_s = \frac{\omega_s}{p_s^{(P)}}\log\left(\frac{\delta_s^{(I)}}{\delta_s^{(P)}}\right),\ \eta_s = \delta_s^{(P)}\left(\frac{\delta_s^{(I)}}{\delta_s^{(P)}}\right)^{\omega_s} \quad (3)$$

B. Joint Medium Access and Rate Allocation

In this work, we don't specify any MAC protocol. Instead we abstract the MAC layer operation through some parameters a_l, ϵ_m and the concept of maximal cliques from graph theory. We first define an abstract MAC layer parameter $a_l \in [0,1]$ which describes the percent of the physical link capacity c_l used by the MAC layer on any link l for the transmission of the upper layer data. In other words, the link can not be used for the transmission during $1-a_l$ percent of the time due to either the capture of medium by another link or the MAC layer overhead such as collisions, control messages, header overhead. Hence the effective MAC layer capacity is $a_l c_l$ and we can now write the *rate constraint* for any link l in the network as $\sum_{r\in\mathcal{R}} h_{l,r}x_r \le a_l c_l$ for entries $h_{l,r}$ of the routing matrix where $h_{l,r}=1$ denotes that the link l is part of the route r and 0 otherwise. The constraint can alternatively be written as $\sum_{r\in\mathcal{R}} h_{l,r}x_r/c_l \le a_l$ for $c_l \ge 0$.

For the medium access part, let M denotes the total number of maximal cliques. Each link is a member of one or more maximal cliques and links in the same clique can not be active at the same time. Hence, using this local conflict information provided by maximal cliques we construct the global conflict matrix F of dimension $M \times L$ where entries $f_{m,l}$ are equal to 1 if link l is a member of clique m, and 0 otherwise. Finally we define a parameter $\epsilon_m \in [0,1]$ specific to the employed MAC protocol which could be calculated a priori as a function of the number of conflicting links given by $f_{m,l}$. It describes the usable percent of the medium within maximal clique m during which links in m can use the medium to transmit data. Hence, in each maximal clique m, the sum of medium access probabilities a_l for conflicting links should satisfy $\sum_{l\in\mathcal{L}} f_{m,l}a_l \le \epsilon_m$. Then by replacing a_l with rate constraint, we obtain; *joint rate allocation and medium access constraint* as $\sum_{l\in\mathcal{L}}\sum_{r\in\mathcal{R}} f_{m,l}\left(h_{l,r}x_r/c_l\right) \le \epsilon_m$. Note that we assume link capacities c_l and entries $h_{l,r}$, $f_{m,l}$ for routing and conflict matrices are constant throughout the optimization.

C. Power-Lifetime Control

In this section, we introduce communication power model and then combine it with the processing power p_s (normalized) in Section II-A to form the power-lifetime control mechanism. For the communication power, we define $\xi_{n,l}$ as the energy consumed per bit on link l of node n where $P_{tx,l}$ and $P_{rx,l}$ are given to be the transmitter and receiver power respectively.

$$\xi_{n,l} = \begin{cases} P_{tx,l}/c_l & \text{, if } l \text{ is an outgoing link of node } n \\ P_{rx,l}/c_l & \text{, if } l \text{ is an incoming link of node } n \\ 0 & \text{, otherwise.} \end{cases} \quad (4)$$

Later for the processing power part, we define the variable $q_{n,s}$ where $q_{n,s}=1$ indicates sensor node n is a source sensor s and $q_{n,s}=0$ otherwise. Note that we allow single video source per node. Then, combining the communication and sensor power, the average power dissipation at node n is $\bar{p}_n = \sum_r \sum_l \xi_{n,l}\, h_{l,r}\, x_r + \sum_{s\in S} q_{n,s}p_s$. Let each node n have an initial energy j_n and the lifetime is given by $T_n = \frac{j_n}{\bar{p}_n}$. We assume any node n runs out of battery results in the failure of the whole network. Hence, we define the network lifetime as the network's operation time until any of the node's energy is depleted and given by $T_{\min} = \min\{T_n | n=1,\cdots N\}$. Let $v = 1/T_{\min}$ be the inverse network lifetime, then lifetime of each node n satisfies $T_n \ge 1/v$. We define $e_{n,r}=\sum_l \xi_{n,l}h_{l,r}$ to simplify the notation where $e_{n,r}$ is node n's total communication energy consumption per bit for flow x_r. Then we have the *power constraint* as $\sum_{r\in\mathcal{R}} e_{n,r}x_r + \sum_{s\in S} q_{n,s}p_s \le j_n v$ where $e_{n,r}$, $q_{n,s}$ and j_n are constants and available only to node n.

D. Quality-Lifetime Maximization Problem

In this section we introduce the quality-lifetime maximization problem for WVSNs. The objective of the problem has two parts. The first part maximizes the *lifetime* of the network where the second part provides the best total sensor-to-sink signal SNR as a measure of *quality* for the compressed video. In the first part, network lifetime is maximized by minimizing the inverse lifetime v given in Section II-C through a convex utility function $g(v)=v^2/2\theta$ for some constant θ. In the second part, higher quality is achieved by increasing peak signal-to-noise-ratio (PSNR) of the received signal from source s at sink, which is given by $\text{PSNR}_s=10\log_{10}(\frac{255^2}{D_s(p_s,y_s)})$. The max. total quality $\sum_s \text{PSNR}_s$ is achieved at the min. of $f(\mathbf{p},\mathbf{x}) = \sum_s d_2 \log(D_s(p_s,y_s))$ where $d_2=10/\log(10)$ and $y_s = \sum_{r\in\mathcal{R}(s)} x_r$. After replacing $D_s(p_s,y_s)$ with (2) and

defining $K = d_2 \sum_s \log(\eta_s)$, we write the objective function to be minimized as $f(\mathbf{p},\mathbf{x})$=K−$f_1(\mathbf{p})$−$f_2(\mathbf{x})$ for functions $f_1(\mathbf{p})$ in (5) and $f_2(\mathbf{x})$=$d_1 d_2 \sum_s \sum_{r\in\mathcal{R}(s)} x_r$. Considering single video source per node assumption (i.e. any route r carry only one source's data), we rewrite $f_2(\mathbf{x})$ as in (5).

$$f_1(\mathbf{p}) = d_2 \sum_s \kappa_s p_s \quad ; \quad f_2(\mathbf{x}) = d_1 d_2 \sum_{r\in\mathcal{R}} x_r \tag{5}$$

Considering the power constraint in Sec. II-C and the joint rate allocation and medium access constraint in Sec. II-B, the quality-lifetime maximization problem is formulated as below. where the original problem is $\mathcal{P}^* = \hat{\mathcal{P}}^* + K$.

$$\hat{\mathcal{P}}^* = \min_{\mathbf{p},\mathbf{x},v} g(v) - f_1(\mathbf{p}) - f_2(\mathbf{x}) \tag{6}$$

$$\text{s.t.} \sum_{r\in\mathcal{R}} e_{n,r} x_r + \sum_{s\in S} q_{n,s} p_s \le j_n v \ , \ \forall n \in \mathcal{N} \tag{7}$$

$$\sum_{l\in\mathcal{L}} \sum_{r\in\mathcal{R}} f_{m,l}\big(h_{lr}/c_l\big) x_r \le \epsilon_m \ , \ \forall m \in \mathcal{M} \tag{8}$$

$$p_{\min} \le p_s \le p_{\max} \ ; \ x_{\min} \le x_r \le x_{\max} \ ; \ v_{\min} \le v \le v_{\max} \tag{9}$$

Dual based methods are desirable to solve this problem since they are easily converted into distributed algorithms and the inherent pricing mechanism is easy to interpret. However due to the lack of strict convexity of the primal problem, dual problem may not be differentiable at every point. To avoid these problems we use Proximal Point Algorithm [8]. Furthermore by conducting a detailed convergence analysis, we provide exact bounds on step sizes which leads to a better understanding of the interactions between the convergence of the algorithm and the network parameters.

III. Dual-based Distributed Quality-Lifetime Maximization Algorithm

In this section we develop a dual-based distributed algorithm based on the *proximal point algorithm* to solve the quality-lifetime maximization problem given in (6)-(9). For that purpose we use the matrix based notation where $\mathbf{H}$, $\mathbf{E}$, $\mathbf{Q}$ and $\mathbf{F}$ are the matrices with entries $h_{l,r}$, $e_{n,r}$, $q_{n,s}$ and $f_{m,l}$ respectively, $\mathbf{C}$=diag$(c_1,\dots,c_L)$ is the capacity matrix and $\mathbf{x} = [x_1 \dots x_R]^T$, $\mathbf{p}$=$[p_1 \dots p_S]^T$, $\boldsymbol{\epsilon}$=$[\epsilon_1 \dots \epsilon_M]^T$, $\mathbf{j}$=$[j_1 \dots j_N]^T$, $\boldsymbol{\kappa}$=$[\kappa_1 \dots \kappa_S]^T$, $\boldsymbol{\eta}$=$[\eta_1 \dots \eta_S]^T$ are the vectors.

Let, the optimal values of the original problem in (6)-(9) be given by $\mathbf{p}^*$=$[p_1^* \dots p_S^*]^T$ and $\mathbf{x}^*$=$[x_1^* \dots x_R^*]^T$, Then we introduce new variables $\hat{\mathbf{p}}$=$[\hat{p}_1 \dots \hat{p}_S]^T$, $\hat{\mathbf{x}}$=$[\hat{x}_1 \dots \hat{x}_R]^T$, and constants V_{ps}, V_{xr} which are used to obtain the additional quadratic terms $\frac{1}{2}\sum_s V_{ps}(p_s-\hat{p}_s)^2$ and $\frac{1}{2}\sum_r V_{xr}(x_r-\hat{x}_r)^2$ to the objective function in (6). These quadratic terms do not effect the original optimal point since the optimal values for new variables are similarly achieved at $\hat{\mathbf{p}}^*$=$\mathbf{p}^*$ and $\hat{\mathbf{x}}^*$=$\mathbf{x}^*$. Then we represent these quadratic terms in matrix notation after defining diagonal matrices $\mathbf{V}_p$=diag$(V_{p1} \dots V_{pS})$, $\mathbf{V}_x$=diag$(V_{x1} \dots V_{xR})$ and using following norm definitions.

$$||\mathbf{p}-\hat{\mathbf{p}}||_{V_p} = (\mathbf{p}-\hat{\mathbf{p}})^T \mathbf{V}_p (\mathbf{p}-\hat{\mathbf{p}}) \tag{10}$$

$$||\mathbf{x}-\hat{\mathbf{x}}||_{V_x} = (\mathbf{x}-\hat{\mathbf{x}})^T \mathbf{V}_x (\mathbf{x}-\hat{\mathbf{x}}) \tag{11}$$

Finally we rewrite the original problem as follows which is to be distributively solved by using proximal point algorithm and dual-based methods.

$$\min_{\substack{\mathbf{p},\mathbf{x},v,\\ \hat{\mathbf{p}},\hat{\mathbf{x}}}} g(v) - f_1(\mathbf{p}) - f_2(\mathbf{x}) + \frac{1}{2}||\mathbf{p}-\hat{\mathbf{p}}||_{V_p} + \frac{1}{2}||\mathbf{x}-\hat{\mathbf{x}}||_{V_x} \tag{12}$$

$$\text{s.t. } \mathbf{E}\mathbf{x} + \mathbf{Q}\mathbf{p} \le \mathbf{j}v \tag{13}$$

$$\mathbf{F}\mathbf{C}^{-1}\mathbf{H}\mathbf{x} \le \boldsymbol{\epsilon} \tag{14}$$

$$\mathbf{p}_{\min} \le \mathbf{p} \le \mathbf{p}_{\max} \ ; \ \mathbf{0} \le \mathbf{x} \le \mathbf{x}_{\max} \ ; \ v_{\min} \le v \le v_{\max} \tag{15}$$

After relaxing constraints (13) and (14) with $\boldsymbol{\mu}$=$[\mu_1 \dots \mu_N]^T \in \mathbf{R}_+^N$ for each node and $\boldsymbol{\psi}$=$[\psi_1 \dots \psi_M]^T \in \mathbf{R}_+^M$ for each max. clique, we write the Lagrangian as below.

$$\hat{L}(\mathbf{p},\mathbf{x},v,\boldsymbol{\mu},\boldsymbol{\psi};\hat{\mathbf{p}},\hat{\mathbf{x}}) = g(v) - f_1(\mathbf{p}) - f_2(\mathbf{x}) + \frac{1}{2}||\mathbf{p}-\hat{\mathbf{p}}||_{V_p}$$
$$\frac{1}{2}||\mathbf{x}-\hat{\mathbf{x}}||_{V_x} + \boldsymbol{\mu}^T\mathbf{E}\mathbf{x} + \boldsymbol{\mu}^T\mathbf{Q}\mathbf{p} - \boldsymbol{\mu}^T\mathbf{j}v + \boldsymbol{\psi}^T\mathbf{F}\mathbf{C}^{-1}\mathbf{H}\mathbf{x} - \boldsymbol{\psi}^T\boldsymbol{\epsilon} \tag{16}$$

In (16), after replacing $f_1(\mathbf{p})$, $f_2(\mathbf{x})$ with (5) and $g(v)$=$v^2/2\theta$ the Lagrangian becomes separable over $\mathbf{p}$, $\mathbf{x}$ and written as $\sum_s \hat{L}_p(p_s,\boldsymbol{\mu};\hat{p}_s) + \sum_r \hat{L}_x(x_r,\boldsymbol{\mu},\boldsymbol{\psi};\hat{x}_r) + \hat{L}_v(v,\mu) - \boldsymbol{\psi}^T\boldsymbol{\epsilon}$ in terms of the partial Lagrangians below.

$$\hat{L}_p(p_s,\boldsymbol{\mu};\hat{p}_s) = \sum_n \mu_n q_{ns} p_s - d_2\kappa_s p_s + \frac{V_{ps}}{2}(p_s-\hat{p}_s)^2 \tag{17}$$

$$\hat{L}_x(x_r,\boldsymbol{\mu},\boldsymbol{\psi};\hat{x}_r) = \sum_n \mu_n e_{nr} x_r + \sum_m \sum_l \psi_m f_{ml} \frac{h_{lr}}{c_l} x_r$$
$$- d_1 d_2 x_r + \frac{V_{xr}}{2}(x_r-\hat{x}_r)^2 \tag{18}$$

$$\hat{L}_v(v,\boldsymbol{\mu}) = v^2/2\theta - \sum_n \mu_n j_n v \tag{19}$$

Then the dual-based solution for the problem in (6)-(9) is obtained by first finding the dual function $D(\boldsymbol{\mu},\boldsymbol{\psi}) = \min_{\mathbf{p},\mathbf{x},v,\hat{\mathbf{p}},\hat{\mathbf{x}}} \hat{L}(\mathbf{p},\mathbf{x},v,\boldsymbol{\mu},\boldsymbol{\psi};\hat{\mathbf{p}},\hat{\mathbf{x}})$, and then maximizing it $\hat{\mathcal{P}}^* = \max_{\boldsymbol{\mu},\boldsymbol{\psi}} D(\boldsymbol{\mu},\boldsymbol{\psi})$. Hence we solve this dual problem by maximizing the concave dual function using gradient descent algorithm (20)-(21) for step sizes $\mathbf{A}_\mu = \text{diag}(\alpha_{\mu 1},\dots,\alpha_{\mu N})$ and $\mathbf{A}_\psi = \text{diag}(\alpha_{\psi 1},\dots,\alpha_{\psi M})$.

$$\boldsymbol{\mu}(t+1) = \big[\boldsymbol{\mu}(t) + \mathbf{A}_\mu(\mathbf{E}\mathbf{x}+\mathbf{Q}\mathbf{p}-\mathbf{j}v)\big]^+ \tag{20}$$

$$\boldsymbol{\psi}(t+1) = \big[\boldsymbol{\psi}(t) + \mathbf{A}_\psi(\mathbf{F}\mathbf{C}^{-1}\mathbf{H}\mathbf{x}-\boldsymbol{\epsilon})\big]^+ \tag{21}$$

In the proximal point algorithm, we first assume the variables $\hat{\mathbf{p}}$ and $\hat{\mathbf{x}}$ as constant and calculate the minimizer $[\mathbf{p}^0(t),\mathbf{x}^0(t),v(t)]$=$\text{argmin}_{\mathbf{p},\mathbf{x},v} \hat{L}(\mathbf{p},\mathbf{x},v,\boldsymbol{\mu}(t),\boldsymbol{\psi}(t);\hat{\mathbf{p}}(t),\hat{\mathbf{x}}(t))$, then make the dual updates (20)-(21) using $(\mathbf{p},\mathbf{x},v) = (\mathbf{p}^0(t),\mathbf{x}^0(t),v(t))$ and find minimizer $(\mathbf{p}^1(t),\mathbf{x}^1(t),v(t+1)) = \text{argmin}_{\mathbf{p},\mathbf{x},v} \hat{L}(\mathbf{p},\mathbf{x},v,\boldsymbol{\mu}(t+1),\boldsymbol{\psi}(t+1);\hat{\mathbf{p}}(t),\hat{\mathbf{x}}(t))$. Finally the proximal point parameters are updated in the direction of the primal variables using (22)-(23) with step sizes $\mathbf{B}_{\hat{p}} = \text{diag}(\beta_{\hat{p}1},\dots,\beta_{\hat{p}S})$ and $\mathbf{B}_{\hat{x}} = \text{diag}(\beta_{\hat{x}1},\dots,\beta_{\hat{x}R})$.

$$\hat{\mathbf{p}}(t+1) = \hat{\mathbf{p}}(t) + \mathbf{B}_{\hat{p}}(\mathbf{p}^1(t) - \hat{\mathbf{p}}(t)) \tag{22}$$

$$\hat{\mathbf{x}}(t+1) = \hat{\mathbf{x}}(t) + \mathbf{B}_{\hat{x}}(\mathbf{x}^1(t) - \hat{\mathbf{x}}(t)) \tag{23}$$

Hence the distributed quality-lifetime maximization algorithm based on proximal point method is given in Table I. This

TABLE I
DUAL-BASED DISTRIBUTED QUALITY-LIFETIME MAXIMIZATION

Initialize: Set $t=0$ and initialize $v(t)$, $\mu_n(t)$, $\psi_m(t)$, $\hat{p}_s(t)$ and $\hat{x}_r(t)$.

A.1. Algorithm for Source Nodes :

Each video source calculates $p_s^0(t)$, $x_r^0(t)$ $\forall r\in\mathcal{R}(s)$ by solving (17), (18)

$$p_s^0(t) = \hat{p}_s(t) + \frac{1}{V_{ps}}\Big(d_2\kappa_s - \sum_n q_{ns}\mu_n(t)\Big)$$

$$x_r^0(t) = \hat{x}_r(t) + \frac{1}{V_{xr}}\Big(d_1 d_2 - \sum_n e_{nr}\mu_n(t) - \sum_m\sum_l f_{ml}\frac{h_{lr}}{c_l}\psi_m(t)\Big)$$

Video sensor s encodes using $\sigma_s(t)=\omega_s(1-p_s^0(t)/p_s^{(P)})$ and total rate $\sum_{r\in\mathcal{R}(s)}x_r^0(t)$. Transmits according to rate allocation $x_r^0(t), \forall r\in\mathcal{R}(s)$

A.2. Algorithm for All Communicating Nodes :

Each node n updates power and conflict prices $\mu_n(t)$, $\psi_m(t)$ using (20)-(21). After properly weighting, send them to sink with min. comm. cost.

$$\mu_n(t+1)=\Big[\mu_n(t)+\alpha_{\mu n}\big(\sum_r e_{nr}x_r^0(t) + \sum_s q_{ns}p_s^0(t) - j_n v(t)\big)\Big]^+$$

$$\psi_m(t+1)=\Big[\psi_m(t)+\alpha_{\psi m}\big(\sum_l\sum_r f_{ml}\frac{h_{lr}}{c_l}x_r^0(t)-\epsilon_m\big)\Big]^+$$

A.3. Sink Algorithm:

Calculates $v(t+1)=\theta\sum_n j_n\mu_n(t+1)$ from (19) and feeds back to sources

A.4. Sensor Algorithm (Source):

Each source calculates $p_s^1(t)$, $x_r^1(t)$ for new values of $\boldsymbol{\mu}(t+1)$, $\boldsymbol{\psi}(t+1)$

$$p_s^1(t) = \hat{p}_s(t+1) + \frac{1}{V_{ps}}\Big(d_2\kappa_s - \sum_n q_{ns}\mu_n(t+1)\Big)$$

$$x_r^1(t) = \hat{x}_r(t) + \frac{1}{V_{xr}}\Big(d_1 d_2 - \sum_n e_{nr}\mu_n(t+1) - \sum_m\sum_l f_{ml}\frac{h_{lr}}{c_l}\psi_m(t+1)\Big)$$

Using (22)-(23) and entities $p_s^1(t)$, $x_r^1(t)$, each source locally updates

$$\hat{p}_s(t+1) = \hat{p}_s(t) + \beta_{\hat{p}s}(p_s^1(t) - \hat{p}_s(t))$$
$$\hat{x}_r(t+1) = \hat{x}_r(t) + \beta_{\hat{x}r}(x_r^1(t) - \hat{x}_r(t))$$

A.5. If converges stop, otherwise set time $t=t+1$ and continue with A.1

low cost algorithm is synchronous and runs once at each time slot t. Steps of the algorithm are designed to run on specific nodes such as source, sink or all communicating sensor nodes. A source node is always both a source and a communicating node, and runs the relevant steps in the given order.

In step A.1 of the algorithm, $p_s^0(t)$ and $x_r^0(t)$ are calculated by using prices $\mu_n(t)$, $\psi_m(t)$ and parameters $\hat{p}_s(t)$, $\hat{x}_r(t)$. After calculating encoder power $p_s^0(t)$ and rates $x_r^0(t)$, video encoder of source s starts encoding by using the I-coding rate given by $\sigma_s = \omega_s(1 - p_s^0(t)/p_s^{(P)})$ and total encoder bit rate $y_s(t)=\sum_{r\in\mathcal{R}(s)} x_r^0(t)$. Then the video data is transmitted on each route according to the rate allocation policy $x_r^0(t)$. In step A.2 each node n updates their power price $\mu_n(t+1)$, by using the flow rates $x_r^0(t)$ on routes traversing node n, encoder power $p_s^0(t)$ (if there is any) and network lifetime $1/v(t)$. On the other hand, the conflict price $\psi_m(t+1)$ is calculated for all max. cliques m associated with the links of node n. However this update requires the link utilization information from the other links l' in the same max. clique m (max. 2-hop), which is given by $\sum_r \frac{h_{l',r}x_r^0(t)}{c_{l'}}$. We note that in steps A.1, A.3 and A.4, the expressions require the weighted sum of these prices (for ex. $\sum_n e_{nr}\mu_n(t+1)$). At each node n by successively adding the weighted prices we obtain weighted sums of the prices at the sink with only minor communication overhead. In this way the prices are obtained at the sink and used in A.3

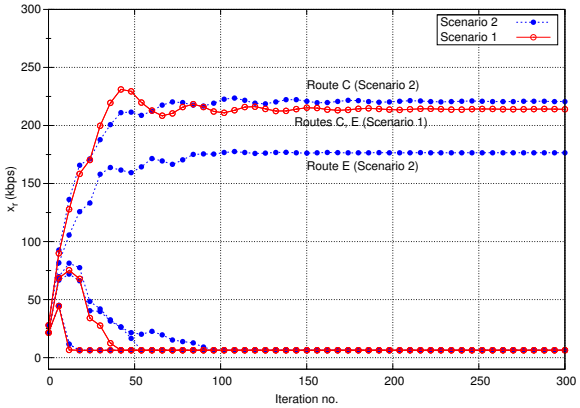

Fig. 2. Convergence of the algorithm for variable x_r

to calculate inverse network lifetime $v(t+1)$. Sink sends this information $v(t+1)$ and weighted sum of the prices back to the sources over the same routes, which are used by sources in steps A.1 and A.4.

Before the end of this section, we provide the following main theorem on convergence which specifies the bounds on step sizes. The proof is given in the Appendix. Note that $\sum_m f_{ml}$ and $\sum_r h_{lr}$ respectively refer to the number of max. cliques for link l and the number of routes using link l. Then we define, $L_{\mathcal{R}}=\max_r\sum_l(h_{lr}/c_l)\sum_m f_{ml}$, $L_{\mathcal{M}}=\max_m\sum_l(f_{ml}/c_l)\sum_r h_{lr}$, $E_{\mathcal{R}}=\max_r\sum_n e_{nr}$, $E_{\mathcal{N}}=\max_n\sum_r e_{nr}$, and $J_T=\sum_n j_n$.

Theorem 1 *The dual-based distributed quality-lifetime maximization algorithm (i.e. Table I) converges to a stationary point for the following conditions on step sizes $\alpha_{\psi m}$, $\alpha_{\mu n}$ and the proximal point algorithm parameters V_{xr}, V_{ps}.*

$$\min_m\left[\frac{1}{\alpha_{\psi m}}\right] \geq 2L_{\mathcal{R}}L_{\mathcal{M}}\max_r\left[\frac{1}{V_{xr}}\right] \quad (24)$$

$$\min_m\left[\frac{1}{\alpha_{\mu m}}\right] \geq \max_s\left[\frac{1}{V_{ps}}\right] + 2E_{\mathcal{R}}E_{\mathcal{N}}\max_r\left[\frac{1}{V_{xr}}\right] + \theta J_T\max_n j_n \quad (25)$$

IV. SIMULATION RESULTS

For the simulations we use the simple topology given in Fig 1(a). Nevertheless it can easily scale up to larger networks since the algorithm is distributed. In the given network, we have N=6 nodes, L=7 links, S=4 sources $\mathcal{S}=\{C,D,E,F\}$ and R=6 routes $\mathcal{R}=\{C, D1, D2, E, F1, F2\}$. We assume a basic MAC scheme in [9] which adapts CSMA range for a given power and communication range d. Hence there are M=3 maximal cliques with $\mathcal{M}=\{\{L1,L2,L4,L5,L7\}, \{L1,L3,L4,L5,L7\}, \{L2,L4,L5,L6,L7\}\}$. We set the distances between adjacent nodes to 50 m. Transmit and receive power of all links are set to P_{tx}=2.5 and P_{rx}=1.2mW. respectively. Hence, assuming SNR=8 dB, coding gain K_c=2 and bandwidth W=250 KHz on all channels, link capacities are found as $\mathbf{c}=[652\ 652\ 475\ 735\ 735\ 475\ 735]^T$ Kbps by $c_l \approx W\log(K_c\text{SINR}_l)$. Finally we assign initial energy of j_n=2 j. for each node and video encoder power of $p_s^{(I)}$=4 mW. and $p_s^{(I)}$=20 mW for each source. We assume all video encoders

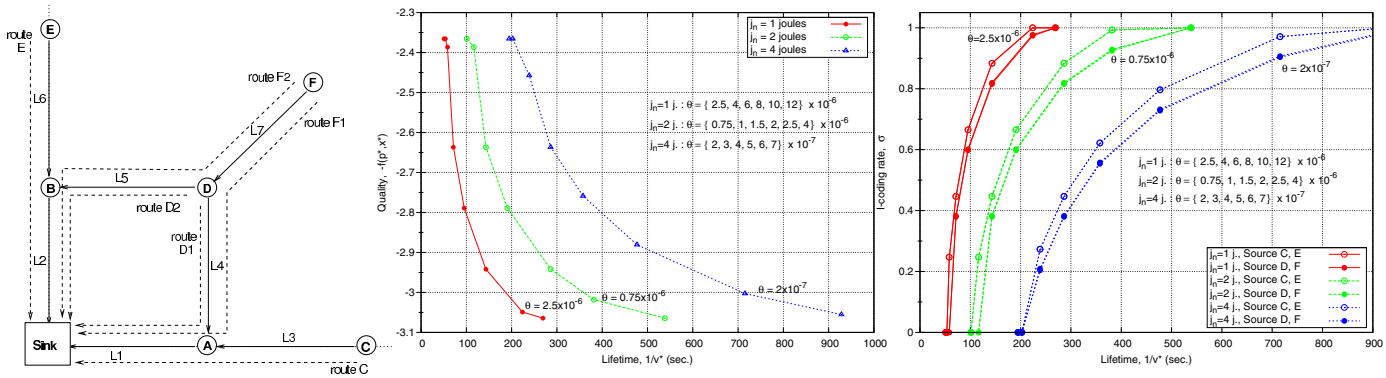

Fig. 1. (a) Topology. (b) Quality-lifetime and (c) video encoder control with the adjustment of θ

are encoding at QCIF resolution at 5 frame/s at a minimum rate of $y_{\min}$. Finally β_ψ=β_μ=1, V_p=V_x=50 and unless otherwise stated θ=2×10^{-6}. Given the above values, we may decide the entities $E_{\mathcal{R}}$=1.7×10^{-3}, $E_{\mathcal{N}}$=2×10^{-3}, $L_{\mathcal{R}}$=1.423, $L_{\mathcal{M}}$=2.2 and J_T=12 which are used to find the bounds $\alpha_\psi \leq 7.98$ and $\alpha_\mu \leq 49.88$ using Theorem. 1.

In all experiments we use $\mathcal{S}$=$\{C, D, E, F\}$ and allow these nodes to capture, compress and transmit video data. In the first experiment we illustrate the convergence of the algorithm and describe two scenarios. The first one is with the default parameters set as mentioned above. However, in the second one we assume link L6's SNR drops to 5.78 dB when transmit power is reduced to $0.6P_{tx}$. From Fig. 2 we observe that in both cases the distributed algorithm converges very fast. We also note that at the optimum, highest rates are assigned to sensors C and E which have completely disjoint paths and causing minimum contention for the medium. And due to the symmetry in the network, exactly the same rates (214 kbps) are allocated by the nodes C and E. However the second scenario is not symmetric, and in this case path from sensor E with the low SNR link L6 is used less and some extra rate is allocated in the other path. These experiments illustrate that the algorithm could react to changes in the network such as routes, link capacities, etc. and seeks the new optimum.

In the second experiment, we observe how the algorithm makes the quality vs. lifetime tradeoff by optimally adapting the encoder power and the rate allocation parameters. We run the algorithm for different initial sensor energies which are set to the same $j_n, \forall n \in \mathcal{N}$ for all nodes. We run for 3 different energy levels $j_n = 1, 2$ and 4 joules. Each experiment is run for a different set of θ values which is simply used to find different trade-off policies between network lifetime and quality as illustrated in Fig. 1(b). Note that the θ values used for each case is listed in the figures. For convenience in Fig. 1(b)-(c), we label the points with smallest θ values in each of the three cases. As the sink asks for a longer lifetime, by setting a lower θ, the network could optimally sacrifice from the quality to meet the longer lifetime requirement (or vice versa). This tradeoff is observed in the Fig. 1(b) for all three cases where the network lifetime can be increased up to 4-5 times by changing this θ parameter. To better understand this trade-off, we plot the I-coding rate (σ) of video sensor vs. the lifetime for the same set of θ values Fig. 1(c). In all three cases $j_n = 1, 2, 4$, an increase in lifetime is achieved as a result of higher rate of I-coding at the video encoder. This is the expected behaviour since I-coding is less costly than the P-coding in terms of the power consumption and by prefering it, sensors save power to increase lifetime. As a result we can say that θ is a parameter to manage the network lifetime which jointly controls the video encoder and the rate allocation (per route) through parameters σ_s and x_r respectively.

V. Conclusion

In this paper we proposed a distributed optimal quality-lifetime control algorithm for wireless video sensor networks. The problem is modeled as a GNUM problem by taking into consideration the video encoder parameters, source rates on routes and the channel contention. Results show that distributed optimal quality-lifetime control could be achieved for different policies described by the quality-lifetime tradeoff parameter θ.

As a next step, the algorithm should be tested in more complex scenarios to assess its convergence rate. Furthermore, transmit power control could be integrated to the framework which has a direct impact on both quality and lifetime.

Appendix
Proof of Theorem 1

Due to lack of space we couldn't include the supporting Lemmas 1-5 to prove Theorem. 1. However the reader can find the lemmas and their proofs in [7].

Proof: After defining the following Lyapunov function $U(t) = ||\boldsymbol{\mu}(t)-\boldsymbol{\mu}^*||_{\mathbf{A}_\mu^{-1}}+||\boldsymbol{\psi}(t)-\boldsymbol{\psi}^*||_{\mathbf{A}_\psi^{-1}}+||\hat{\mathbf{p}}(t)-\hat{\mathbf{p}}^*||_{\mathbf{B}_p^{-1}\mathbf{V}_p}+ ||\hat{\mathbf{x}}(t)-\hat{\mathbf{x}}^*||_{\mathbf{B}_x^{-1}\mathbf{V}_x}+\frac{1}{\theta}(v(t)-v^*)^2$, we show the conditions that make $U(t+1)-U(t)\leq 0, \forall t$. We write this difference in terms of the sum of differences $\Delta_\mu+\Delta_\psi+\Delta_v+\Delta_{\hat{p},\hat{x}}$ which are respectively functions of μ, ψ, v as in (27), (30), (34) and $(\hat{p}, \hat{x})$ as given by $\Delta_{\hat{p},\hat{x}} = ||\hat{\mathbf{p}}(t+1)-\hat{\mathbf{p}}^*||_{\mathbf{B}_p^{-1}\mathbf{V}_p}- ||\hat{\mathbf{p}}(t)-\hat{\mathbf{p}}^*||_{\mathbf{B}_p^{-1}\mathbf{V}_p}+ ||\hat{\mathbf{x}}(t+1)-\hat{\mathbf{x}}^*||_{\mathbf{B}_x^{-1}\mathbf{V}_x}- ||\hat{\mathbf{x}}(t)-\hat{\mathbf{x}}^*||_{\mathbf{B}_x^{-1}\mathbf{V}_x}$. First by using Lemma 4 in [7] we write the following inequality for $\Delta_{\hat{p},\hat{x}}$.

$$\Delta_{\hat{p},\hat{x}} \leq \left|\left|\mathbf{p}^1(t)-\hat{\mathbf{p}}^*\right|\right|_{\mathbf{V}_p}-||\hat{\mathbf{p}}(t)-\hat{\mathbf{p}}^*||_{\mathbf{V}_p}+\left|\left|\mathbf{x}^1(t)-\hat{\mathbf{x}}^*\right|\right|_{\mathbf{V}_x}-||\hat{\mathbf{x}}(t)-\hat{\mathbf{x}}^*||_{\mathbf{V}_x} \quad (26)$$

Using definitions of Δ_μ and Δ_ψ in (27), (30), we write (28) and (31) from the generalization of law of cosines to some normed vector space. Then by respectively applying parts 1 and parts 2 of Lemmas 5 and 3 in [7] we obtain (29) and (32):

$$\Delta_\mu = ||\boldsymbol{\mu}(t+1)-\boldsymbol{\mu}^*||_{\mathbf{A}_\mu^{-1}} - ||\boldsymbol{\mu}(t)-\boldsymbol{\mu}^*||_{\mathbf{A}_\mu^{-1}} \quad (27)$$

$$=-||\boldsymbol{\mu}(t+1)-\boldsymbol{\mu}(t)||_{\mathbf{A}_\mu^{-1}}+2(\boldsymbol{\mu}(t+1)-\boldsymbol{\mu}^*)^T\mathbf{A}_\mu^{-1}(\boldsymbol{\mu}(t+1)-\boldsymbol{\mu}(t)) \quad (28)$$

$$\leq-||\boldsymbol{\mu}(t+1)-\boldsymbol{\mu}(t)||_{\mathbf{A}_\mu^{-1}}+2\Big[(\boldsymbol{\mu}(t+1)-\boldsymbol{\mu}^*)^T\mathbf{E}(\mathbf{x}^0(t)-\hat{\mathbf{x}}^*) \quad (29)$$

$$+(\boldsymbol{\mu}(t+1)-\boldsymbol{\mu}^*)^T\mathbf{Q}(\mathbf{p}^0(t)-\hat{\mathbf{p}}^*)-(\boldsymbol{\mu}(t+1)-\boldsymbol{\mu}^*)^T\mathbf{j}(v(t)-v^*)\Big]$$

We replace the terms $(\boldsymbol{\mu}(t+1)-\boldsymbol{\mu}^*)^T\mathbf{E}$, $(\boldsymbol{\mu}(t+1)-\boldsymbol{\mu}^*)^T\mathbf{Q}$, and $(v(t)-v^*)$ in square brackets in (29) respectively by using parts 2, 1, 3 of Lemma 2 (note that $g(v)=v^2/2\theta$).

$$\Delta_\psi = ||\boldsymbol{\psi}(t+1)-\boldsymbol{\psi}^*||_{\mathbf{A}_\psi^{-1}} - ||\boldsymbol{\psi}(t)-\boldsymbol{\psi}^*||_{\mathbf{A}_\psi^{-1}} \quad (30)$$

$$=-||\boldsymbol{\psi}(t+1)-\boldsymbol{\psi}(t)||_{\mathbf{A}_\psi^{-1}}+2(\boldsymbol{\psi}(t+1)-\boldsymbol{\psi}^*)^T\mathbf{A}_\psi^{-1}(\boldsymbol{\psi}(t+1)-\boldsymbol{\psi}(t)) \quad (31)$$

$$\leq-||\boldsymbol{\psi}(t+1)-\boldsymbol{\psi}(t)||_{\mathbf{A}_\mu^{-1}}+2(\boldsymbol{\psi}(t+1)-\boldsymbol{\psi}^*)^T(\mathbf{F}\mathbf{C}^{-1}\mathbf{H}(\mathbf{x}^0(t)-\hat{\mathbf{x}}^*)) \quad (32)$$

Then by using (29), (32) we write $\Delta_\mu + \Delta_\psi$ as below after properly arranging the terms and defining $\mathbf{J}_\theta \triangleq \mathbf{j}\theta\mathbf{j}^T$.

$$\Delta_\mu + \Delta_\psi \leq -||\boldsymbol{\mu}(t+1)-\boldsymbol{\mu}(t)||_{\mathbf{A}_\mu^{-1}} -||\boldsymbol{\psi}(t+1)-\boldsymbol{\psi}(t)||_{\mathbf{A}_\psi^{-1}}$$
$$+2\Big([\nabla_p f_1(\mathbf{p}^1(t))-\nabla_p f_1(\mathbf{p}^*)]^T(\mathbf{p}^0(t)-\hat{\mathbf{p}}^*)-(\mathbf{p}^1(t)-\hat{\mathbf{p}}(t))^T\mathbf{V}_p(\mathbf{p}^0(t)-\hat{\mathbf{p}}^*)$$
$$+[\nabla_x f_2(\mathbf{x}^1(t))-\nabla_x f_2(\mathbf{x}^*)]^T(\mathbf{x}^0(t)-\hat{\mathbf{x}}^*)-(\mathbf{x}^1(t)-\hat{\mathbf{x}}(t))^T\mathbf{V}_x(\mathbf{x}^0(t)-\hat{\mathbf{x}}^*)$$
$$-(\boldsymbol{\mu}(t+1)-\boldsymbol{\mu}^*)^T\mathbf{J}_\theta(\boldsymbol{\mu}(t)-\boldsymbol{\mu}^*)\Big) \quad (33)$$

By using the definition of Δ_v and the result $(v(t)-v^*) = (\boldsymbol{\mu}(t)-\boldsymbol{\mu}^*)^T\mathbf{j}\theta$ obtained from part 3 of Lemma 2 we write:

$$\Delta_v=\frac{1}{\theta}\Big[(v(t+1)-v^*)^2-(v(t)-v^*)^2\Big]=||\boldsymbol{\mu}(t+1)-\boldsymbol{\mu}^*||_{\mathbf{J}_\theta}-||\boldsymbol{\mu}(t)-\boldsymbol{\mu}^*||_{\mathbf{J}_\theta} \quad (34)$$

In the last step to obtain (35), we use the following equality valid for any set of vectors x, y, w, z in some normed vector space $\mathcal{V}$. $||x-w||_A-||y-w||_A=||x-z||_A - ||y-z||_A-2(x-y)^TA(w-z)$. Using this property we properly arrange the $\mathbf{p}$ and $\mathbf{x}$ related terms in (26) with $(\mathbf{p}^1(t)-\hat{\mathbf{p}}(t))^T\mathbf{V}_p(\mathbf{p}^0(t)-\hat{\mathbf{p}}^*)$ and $(\mathbf{x}^1(t)-\hat{\mathbf{x}}(t))^T\mathbf{V}_x(\mathbf{x}^0(t)-\hat{\mathbf{x}}^*)$ terms in (33) and write $\Delta_\mu+\Delta_\psi+\Delta_v+\Delta_{\hat{p},\hat{x}}$ as below:

$$\Delta_\mu+\Delta_\psi+\Delta_v+\Delta_{\hat{p},\hat{x}} \leq -||\boldsymbol{\mu}(t+1)-\boldsymbol{\mu}(t)||_{\mathbf{A}_\mu^{-1}}-||\boldsymbol{\psi}(t+1)-\boldsymbol{\psi}(t)||_{\mathbf{A}_\psi^{-1}}$$
$$+\big|\big|\mathbf{p}^1(t)-\mathbf{p}^0(t)\big|\big|_{\mathbf{V}_p}^-\big|\big|\hat{\mathbf{p}}(t)-\mathbf{p}^0(t)\big|\big|_{\mathbf{V}_p}^+\big|\big|\mathbf{x}^1(t)-\mathbf{x}^0(t)\big|\big|_{\mathbf{V}_x}^-\big|\big|\hat{\mathbf{x}}(t)-\mathbf{x}^0(t)\big|\big|_{\mathbf{V}_x}$$
$$+||\boldsymbol{\mu}(t+1)-\boldsymbol{\mu}(t)||_{\mathbf{J}_\theta}^-2||\boldsymbol{\mu}(t)-\boldsymbol{\mu}^*||_{\mathbf{J}_\theta}+2[\nabla_p f_1(\mathbf{p}^1(t))-\nabla_p f_1(\mathbf{p}^*)]^T(\mathbf{p}^0(t)-\hat{\mathbf{p}}^*)$$
$$+2[\nabla_x f_2(\mathbf{x}^1(t))-\nabla_x f_2(\mathbf{x}^*)]^T(\mathbf{x}^0(t)-\hat{\mathbf{x}}^*) \quad (35)$$

To show the negativeness of (35) we skip the negative terms $-\big|\big|\hat{\mathbf{p}}(t)-\mathbf{p}^0(t)\big|\big|_{\mathbf{V}_p}^-$, $-\big|\big|\hat{\mathbf{x}}(t)-\mathbf{x}^0(t)\big|\big|_{\mathbf{V}_x}^-$ and $-2||\boldsymbol{\mu}(t)-\boldsymbol{\mu}^*||_{\mathbf{J}_\theta}$. Afterwards we replace positive terms $\big|\big|\mathbf{p}^1(t)-\mathbf{p}^0(t)\big|\big|_{\mathbf{V}_p}$ and $\big|\big|\mathbf{x}^1(t)-\mathbf{x}^0(t)\big|\big|_{\mathbf{V}_x}$ with the expressions in Lemma 1 in [7]. On the other hand, gradient terms $[\nabla_p f_1(\mathbf{p}^1(t))-\nabla_p f_1(\mathbf{p}^*)]=0$ and $[\nabla_x f_2(\mathbf{x}^1(t))-\nabla_x f_2(\mathbf{x}^*)]=0$ due to linearity of $f_1(\mathbf{p})$ and $f_2(\mathbf{x})$, hence we can bound them with a positive value as follows.

$$2[\nabla_x f_2(\mathbf{x}^1(t))-\nabla_x f_2(\mathbf{x}^*)]^T(\mathbf{x}^0(t)-\hat{\mathbf{x}}^*)$$
$$\leq\big|\big|\mathbf{E}^T(\boldsymbol{\mu}(t+1)-\boldsymbol{\mu}(t))-\mathbf{F}\mathbf{C}^{-1}\mathbf{H}(\boldsymbol{\psi}(t+1)-\boldsymbol{\psi}(t))\big|\big|_{\mathbf{V}_x^{-1}} \quad (36)$$

Then replacing it in (35) and considering only the non-negative terms in (35) we re-write the convergence condition as below:

$$(\boldsymbol{\mu}(t+1)-\boldsymbol{\mu}(t))^T\big[2\mathbf{E}\mathbf{V}_x^{-1}\mathbf{E}^T+\mathbf{Q}\mathbf{V}_p^{-1}\mathbf{Q}^T+\mathbf{J}_\theta-\mathbf{A}_\mu^{-1}\big](\boldsymbol{\mu}(t+1)-\boldsymbol{\mu}(t))$$
$$+(\boldsymbol{\psi}(t+1)-\boldsymbol{\psi}(t))^T\big[2\mathbf{F}\mathbf{C}^{-1}\mathbf{H}\mathbf{V}_x^{-1}(\mathbf{F}\mathbf{C}^{-1}\mathbf{H})^T-\mathbf{A}_\psi^{-1}\big](\boldsymbol{\psi}(t+1)-\boldsymbol{\psi}(t))$$
$$\leq 0 \quad (37)$$

In order to satisfy the convergence condition in (37) we investigate the bounds on step sizes $\mathbf{V}_p^{-1}$, $\mathbf{V}_x^{-1}$ and $\mathbf{A}_\mu^{-1}$, $\mathbf{A}_\psi^{-1}$ which guarantee the terms in square brackets to be negative semi-definite. For convenience, we define $\mathbf{G} \triangleq \mathbf{F}\mathbf{C}^{-1}\mathbf{H}$ then for any vector $\mathbf{z} = [z_1 \dots z_M]^T$ we need to show the second term in (37) to be $2\mathbf{z}^T\mathbf{G}\mathbf{V}_x^{-1}\mathbf{G}^T\mathbf{z} \leq \mathbf{z}^T\mathbf{A}_\psi^{-1}\mathbf{z}$. We first write the right hand side as $\mathbf{z}^T\mathbf{A}_\psi^{-1}\mathbf{z} = \sum_m(1/\alpha_{\psi m})z_m^2$. For the left hand side after defining $L_\mathcal{R} = \max_r[\sum_m G_{mr}]$ and $L_\mathcal{M} = \max_m[\sum_r G_{mr}]$ where $G_{mr} = \sum_l f_{ml}h_{lr}/c_l$.

$$\sum_r\frac{2}{V_{xr}}\Big[\sum_m G_{mr}z_m\Big]^2 \leq \sum_r\frac{2}{V_{xr}}\Big(\sum_m G_{mr}\Big)\sum_m G_{mr}z_m^2$$
$$\leq 2L_\mathcal{R}\max_r\Big[\frac{1}{V_{xr}}\Big]\sum_m\Big(\sum_r G_{mr}\Big)z_m^2 \leq 2L_\mathcal{R}L_\mathcal{M}\max_r\Big[\frac{1}{V_{xr}}\Big]\sum_m z_m^2$$

Then we obtain $\min_m\big[\frac{1}{\alpha_{\psi m}}\big] \geq 2L_\mathcal{R}L_\mathcal{M}\max_r\big[\frac{1}{V_{xr}}\big]$ in Theorem. 1 to make the second term in (37) negative semi-definite.

Similarly for any vector $\hat{\mathbf{z}} = [\hat{z}_1 \dots \hat{z}_N]^T$ we need to show the first term in (37) to be $\hat{\mathbf{z}}^T\Big[2\mathbf{E}\mathbf{V}_x^{-1}\mathbf{E}^T+\mathbf{Q}\mathbf{V}_p^{-1}\mathbf{Q}^T+\mathbf{J}_\theta\Big]\hat{\mathbf{z}} \leq \hat{\mathbf{z}}^T\mathbf{A}_\mu^{-1}\hat{\mathbf{z}}$ Note that maximum one video source per node is allowed. Then after defining $E_\mathcal{R} = \max_r\big[\sum_n e_{nr}\big]$, $E_\mathcal{N} = \max_n\big[\sum_r e_{nr}\big]$, $J_T = \sum_n j_n$ and $j' = \max_n j_n$, the following bound on step sizes is obtained.

$$\min_m\Big[\frac{1}{\alpha_{\mu m}}\Big] \geq \max_s\Big[\frac{1}{V_{ps}}\Big]+2E_\mathcal{R}E_\mathcal{N}\max_r\Big[\frac{1}{V_{xr}}\Big]+\theta J_T\max_n j_n$$

■

REFERENCES

[1] I. F. Akyildiz, et.al. "A survey on wireless multimedia sensor networks," *Computer Networks*, vol. 51, no. 4, pp.921-960, Mar. 2007.

[2] M. Chiang, et. al., "Layering as optimization decomposition: A mathematical theory of network architectures," *Proc. of the IEEE*, vol. 95, no. 1, pp. 255-312, Jan. 2007.

[3] Y. Lin, et. al. "Optimal joint power-rate adaptation for error resilient video coding," *IS&T/SPIE VCIP*, Jan. 2008.

[4] H. Nama, et.al. "Optimal utility-lifetime trade-off in wireless sensor networks: Characterization and distributed algorithms," *IEEE ICC*, 2006.

[5] Y. F. He, et.al. "Network lifetime maximization in wireless visual sensor networks using a distributed algorithm," *Proc. of IEEE ICME* , 2007.

[6] X. Lin and N. B. Shroff, "Utility maximization for communication networks with multipath routing," *IEEE Trans. on Automatic Control*, vol. 51, no. 5, May 2006.

[7] E. Gurses et. al., "Distributed quality-lifetime maximization in wireless video sensor networks," *Univ. of Waterloo, Tech. Rep. CS-2008-19*, http://www.cs.uwaterloo.ca/research/tr/2008/CS-2008-19.pdf Sep. 2008.

[8] D. P. Bertsekas and J. N. Tsitsiklis *Parallel and Distributed Computation: Numerical Methods*. Upper Saddle River, NJ: Prentice-Hall, 1989.

[9] Y. Yang, J.C. Hou, and L.-C. Kung, "Modeling the effect of transmit power and physical carrier sense in multi-hop wireless networks," *Proc. IEEE INFOCOM*, May 2007.